
This is an electronic reprint of the original article.
This reprint may differ from the original in pagination and typographic detail.

Gallegos Rosas, Katherine; Myllymäki, Pia; Saarniheimo, Mikael; Sneck, Sami; Raju, Ramesh; Soldano, Caterina

Hafnium Aluminate–Polymer Bilayer Dielectrics for Organic Light-Emitting Transistors (OLETs)

Published in:
ACS Applied Electronic Materials

DOI:
[10.1021/acsaelm.3c01813](https://doi.org/10.1021/acsaelm.3c01813)

Published: 27/02/2024

Document Version
Publisher's PDF, also known as Version of record

Published under the following license:
CC BY

Please cite the original version:
Gallegos Rosas, K., Myllymäki, P., Saarniheimo, M., Sneck, S., Raju, R., & Soldano, C. (2024). Hafnium Aluminate–Polymer Bilayer Dielectrics for Organic Light-Emitting Transistors (OLETs). *ACS Applied Electronic Materials*, 6(2), 1493-1503. <https://doi.org/10.1021/acsaelm.3c01813>

This material is protected by copyright and other intellectual property rights, and duplication or sale of all or part of any of the repository collections is not permitted, except that material may be duplicated by you for your research use or educational purposes in electronic or print form. You must obtain permission for any other use. Electronic or print copies may not be offered, whether for sale or otherwise to anyone who is not an authorised user.

Hafnium Aluminate–Polymer Bilayer Dielectrics for Organic Light-Emitting Transistors (OLETs)

Katherine Gallegos-Rosas,* Pia Myllymäki, Mikael Saarniheimo, Sami Sneek, Ramesh Raju, and Caterina Soldano*

Cite This: *ACS Appl. Electron. Mater.* 2024, 6, 1493–1503

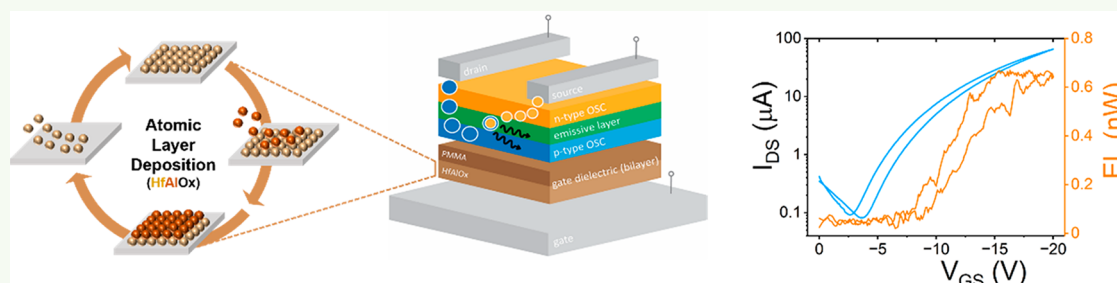
Read Online

ACCESS |

Metrics & More

Article Recommendations

Supporting Information



ABSTRACT: Organic light-emitting transistors are thin-film transistors capable of generating and sensing light under appropriate bias conditions. Achieving a low-voltage operation while maintaining high efficiency can be obtained by using high-mobility semiconductors, highly efficient emissive layers, and high-capacitance dielectrics. We report on the fabrication, dielectric characterization, and implementation of (organic/inorganic) bilayer dielectric stacks in green organic light-emitting transistors. Our dielectric stack includes a nanoscale hafnium aluminate layer fabricated by atomic layer deposition and a thin layer of a polymer dielectric. We found that the hafnium aluminate layer is amorphous in nature and highly transparent in all the visible range. The bilayer stack showed around 10 times higher capacitance per unit area than our polymer reference dielectric. When used as a dielectric in organic light-emitting transistors, this stack enabled low leakage current and operation below 20 V, with a threshold around 6 V and similar efficiencies. Thus, engineering the dielectric layer can enable the tuning of the device working conditions and performances while keeping robustness and negligible leakage values. Thus, these findings open the way to use nanoscale organic/inorganic bilayer dielectrics to enable low-bias, low-power consumption optoelectronic devices of relevance for next-generation electronics applications.

KEYWORDS: organic light-emitting transistor (OLET), bilayer dielectric, high-k dielectric, organic/inorganic dielectric, atomic layer deposition, hafnium aluminate, poly(methyl methacrylate) (PMMA)

INTRODUCTION

In recent years, organic devices, including solar cells (OPV), organic field-effect transistors (OFETs), memories, and organic light-emitting diodes (OLEDs), have been successfully proposed and demonstrated as a new technology platform for high-performance electronic devices, with enormous potentials for cost reduction and new functionalities with respect to current systems based on inorganic materials.¹ In recent years, organic light-emitting transistors (OLETs) have emerged as a promising device platform for fields such as flexible and wearable electronics. OLETs are electrical switches (with channel conduction modulation) capable at the same time of generating and sensing light under appropriate bias conditions.² Differently from the OLED counterpart, light in an organic light-emitting device can be spatially tuned across and within the channel, possibly leading to both top and bottom emissions, without the need of a transparent electrode to extract the light. Characterized by a planar device structure and

charge transport, organic light-emitting transistors are potential candidates for integration into flexible displays, where simplification of manufacturing process at the front-plane level can be envisioned; this can lead to lower costs, reduced production time, and increased yield given the reduced complexity.³

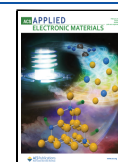
Multilayer OLET structures, where charge transport and light generation can be decoupled and each allocated to different layers to promote exciton confinement in the emissive layer,⁴ show higher current densities and external quantum efficiency (EQE). It has been shown that these devices can

Received: December 22, 2023

Revised: January 2, 2024

Accepted: January 18, 2024

Published: February 2, 2024



outperform equivalent organic light-emitting diodes,⁵ with demonstrated potentials to achieve high luminance (>500 cd/m²) at low voltages (<10 V).^{6,7} Also, device engineering has been proposed to improve overall performances, including for example enhancement of the outcoupling efficiency,⁸ dual gate architectures for a more balanced hole and electron charge transport,⁹ and nonplanar source and drain electrodes to improve charge injection.^{10,11}

When it comes to materials, achieving high-performance OLETs requires high-mobility organic semiconductors (OSCs),¹² high-efficiency luminescent materials,¹³ and high-capacitance gate dielectrics.¹⁴ Further, the interface between the active organic materials and the dielectric layer is key for the overall transistor performance because this is the region where important processes such as charge transport and accumulation occur.²

High-capacitance dielectrics can be achieved by reducing the thickness of the gate dielectric layer or by using dielectric materials with a large dielectric constant (k); this has the overall effect of decreasing operating voltages, thus enabling low-power consumption devices. Oxide dielectrics like SiO₂ have been extensively used in the microelectronics industry; however, continuous miniaturization and dielectric film thickness reduction have led SiO₂ to reach its ultimate physical limit (few nm).¹⁵ Similarly, polymer dielectrics have been widely studied for transistor applications, and they have enabled device fabrication on plastic substrates, relevant for innovative fields such as flexible electronics and wearables. However, it is extremely challenging to fabricate thin polymer dielectric films (<100 nm) with high capacitance, while keeping effective screening of electrodes defects (gate) and high smoothness, which at last can affect leakage currents and breakdown voltages as well as interface quality. Poly(methyl methacrylate) (PMMA) is commonly used as a dielectric in organic field-effect transistors¹⁶ because it enables extremely smooth film formation, favorable for semiconductor growth and leading to good device performance, resulting from the limited number of trap sites at the interface.¹⁴ Along with PMMA, various polymeric materials have been implemented in organic transistors including polyimide,¹⁷ SU-8,¹⁸ and polyvinylphenol (PVP).¹⁹ However, these polymers exhibit low dielectric constant, which prevents low-bias operation.

Furthermore, higher permittivity materials allow fabrication of thicker insulator films while preserving high capacitance values. A large part of the studies on gate dielectrics materials in *field-effect* devices has been dedicated to inorganic materials²⁰ and only more recently to organic transistors.^{21,22} In addition to their dielectric properties, these gate materials are expected to be processable into thin high-quality and *defect-free* films because this can enable transistors operating at low-bias, fast switching speed, and large ON/OFF ratio. Additionally, to be compatible with plastic substrates, gate fabrication and manufacturing should be performed at low deposition temperatures.

In our earlier works, we have developed dielectric films based on high- k poly(vinylidene fluoride) (PVDF)-based polymers and demonstrated that by engineering these films (i.e., polymer composition and its content, solvent, film fabrication parameters), an overall improvement of organic light-emitting transistors optoelectronic properties can be achieved (threshold voltages <20 V with enhanced light output).^{23–25}

Also, metal oxides such as Al₂O₃, HfO₂, and ZrO₂ have been proposed as high- k dielectrics due to their excellent dielectric properties, large bandgap, and optical transparency in the visible region for high-performance and transparent electronic devices.²⁶ Alumina, with dielectric constant k of approximately 7–9,^{27–29} offers several key features, including chemical and thermal stability (amorphous up to 1000 °C),³⁰ good adhesion to various surfaces, and excellent dielectric properties.³¹ Hafnia, with higher dielectric constant (~ 22 – 25), is also chemically stable and highly resistant to corrosive species, while exhibiting biocompatibility³² and barrier properties against moisture; however, it can easily crystallize.^{29,33}

Combining and/or mixing oxides represents a way to tailor the optical and electronic properties of a coating layer for a particular application. This approach can also promote the formation of amorphous structures and lower surface roughness leading to reduction of leakage current density and higher dielectric strength.²⁶ Park et al. have shown that by adding Al₂O₃ into a HfO₂ film, it is possible to achieve a dielectric constant of about 47.³⁴ This value is almost double compared to the reported values for a HfO₂-only film, most likely because of the stabilization of the metastable tetragonal phase of HfO₂. For example, mixed oxides based on Al₂O₃ and TiO₂ have been shown as possible candidates as high-performance gate materials, where their large difference in refractive index between the oxides enables optical coatings with large dielectric permittivity and low leakage currents.³⁵

Atomic layer deposition (ALD) allows for the deposition (at low temperatures) of highly conformal and *defect-free* thin films,³⁶ with high resistivity and good barrier properties³⁷—key features for use as gate insulators. ALD is a surface-driven fabrication process compatible with various substrates and irregular shapes, which can ensure uniformity and control of film thickness over large areas as well as films' composition at the atomic level.³⁸ ALD-grown oxides have been used as dielectric materials in organic field-effect transistors. For example, Zhang et al. used a thick ALD Al₂O₃ film (200 nm) in pentacene-based OFET and demonstrated improved electrical performance, hole mobility of 0.9 cm²/(V s), reduced threshold voltage, and a higher ON/OFF ratio (approximately 1 order of magnitude, when compared to SiO₂-based devices).³⁹ Similarly, bilayer dielectric stacks have also been investigated. For instance, a bilayer composed of ALD layers (Al₂O₃ and HfO₂ nanolaminate) and an amorphous fluoropolymer (CYTOP) has shown improved environmental stability and better performance, including reduction of the threshold voltage (<2 V) and hysteresis, and high mobility values in different OFET configurations.^{40,41} Likewise, FETs fabricated with nanolaminates (i.e., dielectric bilayers composed by Al₂O₃ and HfO₂) in combination with inorganic semiconductors like AlGaIn/GaN or IGZO (indium gallium zinc oxide) showed lower leakage current, smaller threshold voltage, and a higher ON/OFF ratio when compared to single-oxide layers devices.^{30,31,42,43}

Integrating these dielectric materials in organic light-emitting transistors is currently yet not very much studied; however, literature works on (organic) field-effect transistors suggest that using higher capacitance dielectrics (and in particular high- k dielectrics) can expectedly lead to an overall improvement of the device (opto) electronic properties.

In the present work, we study the potential use as gate dielectrics of hafnium aluminate (HfAlO_x) films grown by atomic layer deposition in organic light-emitting transistors. In

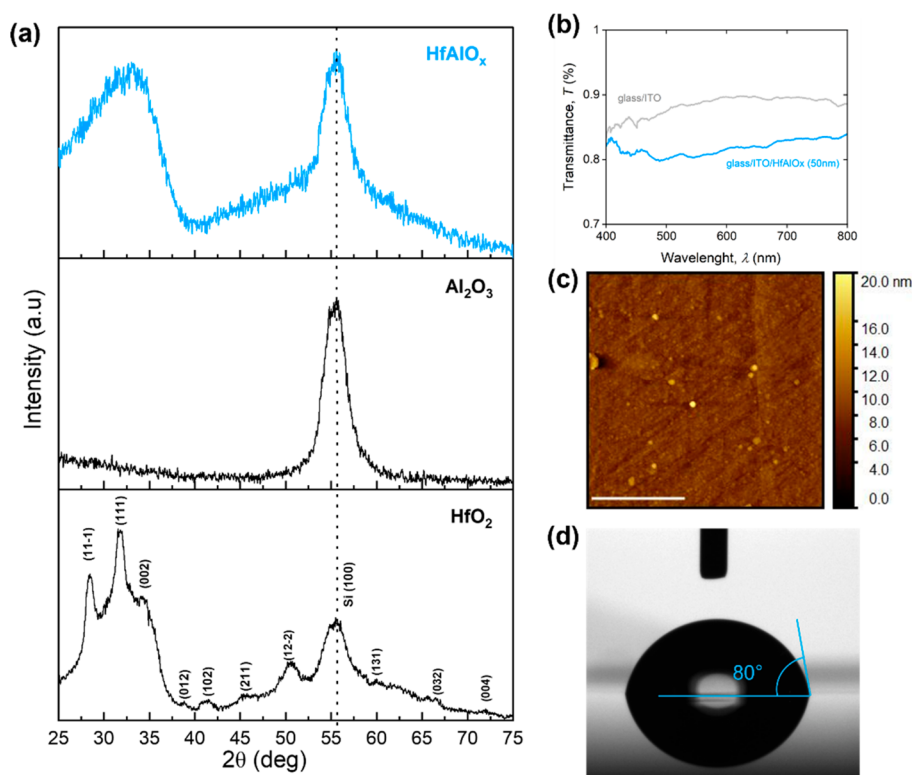


Figure 1. Characterization of HfAlO_x film grown by atomic layer deposition. (a) GIXRD diffractograms (top to bottom) of ALD grown HfAlO_x, Al₂O₃, and HfO₂ films 50 nm thick. (b) Transmittance spectra of HfAlO_x film grown on glass/ITO substrate in the range 400–800 nm. The spectrum of glass/ITO is also included as a reference. (c) Atomic force microscopy (AFM) image of HfAlO_x oxide films (thickness 50 nm) on glass/ITO surface. Scale bar is 2 μm. (d) Contact angle measurement of the HfAlO_x surface (see the text for details).

particular, we study the film composition and surface morphology of this oxide mixture, and we implement it in a bilayer dielectric stack composed of nanoscale hafnium aluminate (mixture of alumina and hafnia) and a PMMA film. We also characterize the optical and dielectric responses of this bilayer dielectric. Such a dielectric stack is then used in organic light-emitting transistors, with the overall effect of considerably reducing driving and threshold voltages, when compared to our standard polymeric dielectric (PMMA-only dielectric). This holds enormous potential for the future development of low-bias, high-performance light-emitting devices.

EXPERIMENTAL SECTION

Materials and Film Preparation. Glass/ITO substrates were cleaned in an ultrasonic bath in diluted Hellmanex III followed by deionized (DI) water, acetone, and 2-propanol as described in our previous work.²⁵ Prior to dielectric polymer deposition, substrates were treated with oxygen plasma (100 W for 15 min).

HfAlO_x films were deposited in a TFS 200 reactor (Beneq Oy, Espoo, Finland) at deposition temperature 250 °C. HyALD (HfCp(NMe₂)₃, >99%, Air Liquide), trimethylaluminum (TMA, >98%, Strem), and deionized water were used as hafnium, aluminum, and oxygen precursors, respectively. HyALD was evaporated from a stainless-steel container heated to 65 °C. TMA and water containers were kept at 20 °C. The metal precursor pulsing ratio was Hf:Al = 2:1. The HfAlO_x deposition sequence consisted of two consecutive cycles of HfO₂ (HyALD + H₂O) followed by one cycle of Al₂O₃ (TMA + H₂O). The growth per HfAlO_x supercycle was 1.57 Å/supercycle, resulting in average growth per cycle (GPC) of 0.52 Å/cycle. Constant nitrogen flow (99.999%, 500 sccm) was used as carrier and purging gas. Silicon pieces were used as additional substrates to monitor film thickness.

Polymer dielectric films were deposited by spin-coating and then annealed for 30 min on a hot plate (110 °C) in ambient conditions. Capacitor-like structures (electrode/dielectric/electrode) were fabricated to evaluate dielectric properties; the dielectric layer is sandwiched between bottom (ITO) and top electrodes (silver, 70 nm).

Film Characterization. The thickness of HfAlO_x films was measured from monitor silicon samples by ellipsometry (Sentech SE400adv ellipsometer) using a wavelength of 633 nm and measuring the angle 70°. The thickness of the polymer dielectric films was measured using a stylus Dektak/XT profilometer (Bruker) with a scan length ~600 μm and a stylus force of 1 mg. The crystal structure of the oxide film was observed by grazing incidence X-ray diffraction (GIXRD, Rigaku SmartLab XRD, Cu Kα radiation, λ = 0.154178 nm). Surface morphology of the films (dielectric and organic layers) was investigated with an atomic force microscope (AFM, Bruker Dimension Icon), with a 5 μm × 5 μm scan size area and resolution of 512 lines/sample. The transmittance was measured with an integrating sphere and a UV–vis spectrometer (Ocean Optics). A probe station connected to (a) an Agilent U1701B capacitance meter was used to measure the static capacitance, and to (b) a semiconductor parametric device analyzer (B1500A Keysight) was used to study C–V, C–f, and dielectric breakdown in capacitor-like structures.

Device Fabrication and Characterization. Organic and metal thin films were deposited using a Moorfield Nanotechnology MiniLab90 instrument (chamber base pressure of 10^{−7} mbar). Electro-optical characteristics of organic light-emitting transistors were measured through a homemade system connected to a semiconductor device analyzer (B1500A Keysight). A photodiode (Hamamatsu S1337) in direct contact with the substrate was used to measure the light output (bottom emission). For further details on standard device fabrication and characterization we refer the reader to ref 25.

RESULTS AND DISCUSSION

Film Properties of Hafnia Aluminate (HfAlO_x) Dielectric Grown by ALD. Several studies in the literature have shown that dielectric properties of high-*k* materials are highly dependent on their stoichiometric composition as well as they are affected by their degree of crystallinity, crystallographic orientation, and crystal structure.⁴⁴ Amorphous and monoclinic phases generally appear at lower (room) temperature, which are preferred phases for semiconductor process; the crystallized phase can be achieved thermodynamically at higher temperatures.⁴⁵ In particular, it has been shown that HfAlO_x film crystallization depends on composition (Al concentration) and on the structure of the film resulting from the deposition cycle sequence.⁴⁶ X-ray diffraction (XRD) is performed to evaluate the structure and growth quality in our films.

Figure 1a shows the GIXRD spectra for (top) HfAlO_x mixture, (middle) HfO₂, and (bottom) Al₂O₃, where all the layers have been grown by atomic layer deposition, and each panel is labeled accordingly. HfO₂ film is polycrystalline, as recognized by XRD studies, and the peak positions clearly indicate the monolithic and tetragonal phases (ICDD PDF-2 card #01-075-6426 and DD PDF-2 card #01-075-6426).⁴⁷ In the Al₂O₃ film, there are no distinctive diffraction peaks except the one identified for the silicon wafer, supporting the amorphous nature of the film. Such a nearly amorphous structure is maintained in the HfAlO_x samples. We found the angle $2\theta = 32^\circ$ with broad width and low intensity; this indicates the presence of very small grains (i.e., nanosized crystallite) locally embedded in the amorphous structures, suggesting that crystallization in the HfAlO_x film is more effectively suppressed than in the pure film (HfO₂).

Figure 1b shows the optical transmittance of the HfAlO_x ALD-grown film (50 nm) deposited on the glass/ITO substrate. Within the visible range (400–800 nm), we found that the nanoscale layer reduces by approximately 10% the transmission of light over the entire visible range, with the overall value remaining above 80% for all wavelengths (see also Figure S1 of the Supporting Information). The optical properties of the film will be relevant later in the article when these films are used as dielectrics in light-emitting devices.

Further, Figure 1c shows the atomic force microscopy (AFM) micrograph of the HfAlO_x film on the ITO/glass substrate (scan size of 5 μm × 5 μm). As expected, the film grown by atomic layer deposition conformably covers the underlying ITO surface. The surface roughness, root-mean-square (rms), is smaller than 3 nm, like ITO on glass (Figure S2). We also investigated the nature of the surface in terms of hydrophobicity/hydrophilicity, which plays an important role in the OSC arrangement on the surface and, thus, affects the interface between the dielectric and organic semiconductor (OSC) layers.⁴⁸ It is well-known that the oxide layer presents dangling bonds on the surface, which can affect the deposition of organic molecules on top as well as the charge transport properties. The HfAlO_x film shows a contact angle of approximately 80° (Figure 1d), which suggests a more hydrophobic surface nature compared to polymeric dielectric (approximately 65° for PMMA layer; see Figure S3).

Dielectric Response of Bilayer Dielectrics (HfAlO_x/PMMA). Previous works^{49,50} have shown that pristine high-*k* oxide films might present a rougher surface⁴⁹ and are prone to higher moisture absorption,²⁷ which can then lead to higher

leakage currents.⁵¹ The interface between the oxide (dielectric) and organic material is strongly dependent on the preparation of the oxide surface; for example, ITO surface treatments can affect the performance of organic light-emitting diodes.⁵² In this work, we selected a bilayer dielectric approach to favor interfacial compatibility at such interface;^{53,49} this consists in the deposition of a thin layer of PMMA on top of the oxide film. PMMA offers a favorable surface for organic semiconductor deposition and growth, is optically transparent, and presents excellent mechanical, chemical, and dielectric properties.⁵⁴ Oxide surfaces were treated with oxygen plasma for 15 min (Tepla 400 system, power of 100 W), before the deposition by spin-coating of the thin PMMA layer (50 nm, MicroChem 950 PMMA). The polymer is then cured on a hot plate at 110 °C for 30 min to remove any residual solvent and water which might affect device performances.⁵⁵

Using a bilayer dielectric reduces the effective permittivity of the overall dielectric stack, resulting from the series capacitor formed by the ALD film and the PMMA layer; however, this is necessary for correct device operation. We found not negligible values of gate leakage currents for transistors fabricated directly on oxide film dielectric (not shown). From now on, we will refer to the device dielectric as the bilayer stack (unless otherwise specified).

Dielectric properties of the bilayer stack were evaluated through capacitor-like structures (electrode/bilayer dielectric/electrode) by sandwiching HfAlO_x/PMMA between the ITO electrode (bottom electrode) and a silver top electrode (70 nm, electrode area ~0.08 cm²), as schematically depicted in Figure 2a.

Eight test capacitors were fabricated, for which we measured average values of the capacitance (per unit area), *C_i*, of about 63 nF/cm². Figure 2b shows the capacitance (per unit area)–voltage (*C_i*–*V*) response of our bilayer dielectric stack (HfAlO_x (50 nm)/PMMA (50 nm)) in the bias range 0–20 V. Corresponding characterization of our optimized test dielectric layer (PMMA, Allresist AR-P 669.09, ~440 nm) is also included as reference. For both dielectrics, we observed no significant variation of the capacitance over the range of biases studied (HfAlO_x/PMMA: 20 V; PMMA: 100 V). Further, we note that this PMMA is different from the PMMA 950 series used in the bilayer stack (solvents are ethyl lactate and anisole, respectively), with the latter one being the polymer of choice because it allows for the deposition of the thinnest layer (50 nm). The capacitance per unit area *C_i* is calculated from

$$C_i = \frac{C}{A} = \frac{k\epsilon_0}{t} \quad (1)$$

where *A* is the electrode area, *t* is the dielectric thickness, and ϵ_0 is the vacuum permittivity (8.85×10^{-12} F/m). The dielectric constant for the bilayer stack at 1 kHz is estimated to be ~7.1, larger than that of the PMMA-only counterpart (*k* ~ 3.3); this value is smaller than the corresponding values for dielectric films made of Al₂O₃ (*k* ~ 7.5–9) and HfO₂ (*k* ~ 17–25). From this, we can also estimate the dielectric permittivity of the individual HfAlO_x layer, which we found to be around 8.5 (see the Supporting Information), consistent with available literature work.⁵⁶

The bilayer stack showed good dielectric strength with no signs of dielectric breakdown up to |20 V|; in the literature, breakdown fields for other similar high-*k* oxides are mostly in the range of 4–5 MV/cm²⁸ (in our case we reach vertical fields of approximately 2 MV/cm). Bilayer stack with thinner oxide

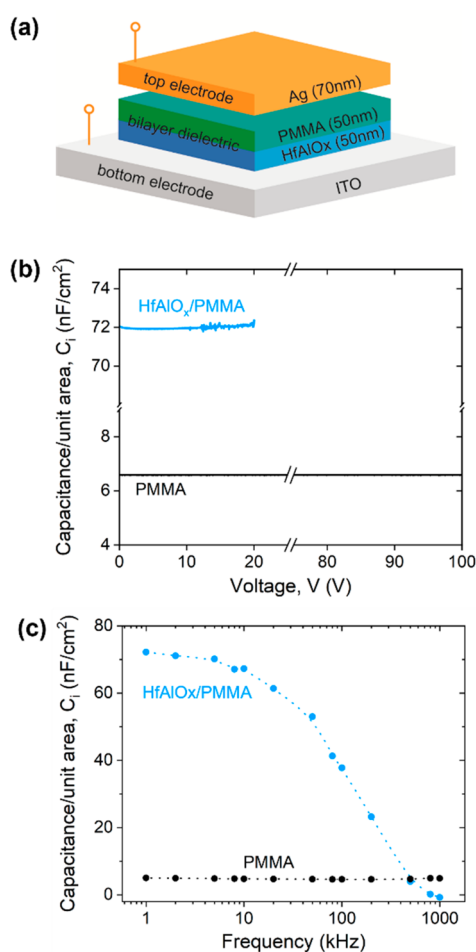


Figure 2. Dielectric characterization of HfAlO_x/PMMA bilayer stack. (a) Schematic of the capacitor-like structure (electrode/dielectric/electrode) where the dielectric is the bilayer stack HfAlO_x (50 nm)/PMMA (50 nm). Capacitance per unit area (b) vs voltage (C_i - V) and (c) vs frequency (C_i - f) for the dielectric stack in (a). Corresponding dielectric characterization for PMMA-only dielectric (440 nm thickness) is also included as reference.

layers (10 and 30 nm) have been also tested and showed either breakdown or high value of leakage current ($> \text{few } \mu\text{A}$), whether an additional PMMA layer is used or not (not shown). Also, the topmost PMMA surface within the bilayer dielectric stack shows a value of surface roughness $r_{\text{rms}} < 3 \text{ nm}$, suggesting that the polymer deposition does not modify the overall morphology of the dielectric stack (see the Supporting Information).

Figure 2c shows the frequency dependence of the capacitance per unit area in the frequency range from 1 kHz to 1 MHz. A DC bias voltage is applied between the bottom (ITO) and the top electrode (silver), with the superimposition of a small AC voltage (30 mV). PMMA-only dielectric capacitance is also shown for comparison; it remains constant within the entire range of frequencies. On the other hand, the bilayer stack shows a constant value up to approximately 10 kHz (suggesting the capacitor stability under a continuously increasing DC voltage stress), followed by a sudden decrease at higher frequency. The observed dielectric relaxation, expectedly occurring mainly in the oxide layer, strongly depends on the polarization response time related to the dipole alignment within the film. In particular, the real part of the dielectric

permittivity ϵ ($C \sim \text{Re}(\epsilon)$) is strongly dependent on the frequency of the alternating electric field. Different polarization mechanisms can occur, including dipole orientation polarization ($\sim 10^2$ – 10^{10} GHz), atomic (10^{12} – 10^{15} Hz), and electronic polarization (10^{15} – 10^{18} Hz). These results are consistent with analogous findings on high- k materials. For low- k materials, as in the case of PMMA-only dielectrics, this change is not significant as the largest contribution to dielectric constant comes presumably from the electronic polarization.²⁷

Organic Light-Emitting Transistors with Bilayer Stack (HfAlO_x/PMMA) Dielectrics. We used a bottom-gate/top-contacts (BG-TC) transistor configuration, as schematically shown in Figure 3a, with the bilayer dielectric stack as the gate dielectric. The device active region consists of an organic multilayer heterostructure, where all layers are thermally evaporated in a vacuum system (Moorfield Nanotechnology MiniLab90) at a base pressure of 1×10^{-7} mbar. The heterostructure includes three stacked organic films, where starting from the bottom: (a) a hole-transporting semiconductor (2,7-dioctyl[1]benzothieno[3,2-*b*][1]benzothiophene, C8-BTBT, 30 nm, Sigma-Aldrich), in direct contact with the dielectric; (b) an emissive layer, where the electron-hole recombination and emission processes take place, is a host-guest matrix system; we used a 10% blend of tris(4-carbazoyl-9-ylphenyl)amine (TCTA) and tris(2-phenylpyridine)iridium(III) (Ir(ppy)₃) (TCTA:Ir(ppy)₃, 60 nm, both from American Dye Source Inc.); (c) an electron-transporting semiconductor (α,ω -diperfluorohexyl-quarterthiophene, DFH-4T, 45 nm, Sigma-Aldrich).

Drain and source electrodes (silver, 70 nm) were thermally evaporated on top of the n-type semiconductor layer. From an energy point of view, this structure enables the efficient injection of charges and diffusion toward the emissive layer (see Figure 3b); in fact, the HOMO level of the p-type semiconductor and the LUMO level of the n-type semiconductor are aligned with the HOMO and the LUMO of the emitter in the emissive layer, respectively. In addition, controlling the interface morphology is highly desirable to enable an efficient conduction path within the semiconductor transport layers. More general considerations on the energetics of this multilayer OLET and materials therein, as well as on the full optoelectronic characterization of the used emissive blend, can be found in ref 57. Figure 3c shows an optical image of a representative substrate containing multiple (8) organic light-emitting transistors (top view). Electrodes and channel are labeled accordingly.

Figure 4 shows the optoelectronic characterization of organic light-emitting transistors using the HfAlO_x/PMMA (50/50 nm) bilayer stack dielectric. Throughout the text, we will refer to these devices as ALD-OLET. These measurements have been performed in a controlled environment (glovebox) to prevent molecular species such as water and oxygen to be adsorbed on the organic layer and on the dielectric surface. Figures 4a and 4c report corresponding curves for a device using PMMA (-only) as the dielectric (440 nm, and referred to as PMMA-OLET), included as reference. PMMA- and ALD-OLET have the same device geometry and structure, with the fabrication process performed at the same time. The electroluminescence (EL) (right y -axis) refers to the light measured through the gate (bottom emission) with a photodiode in direct contact with the substrate. We note that driving bias conditions are different for PMMA- and ALD-

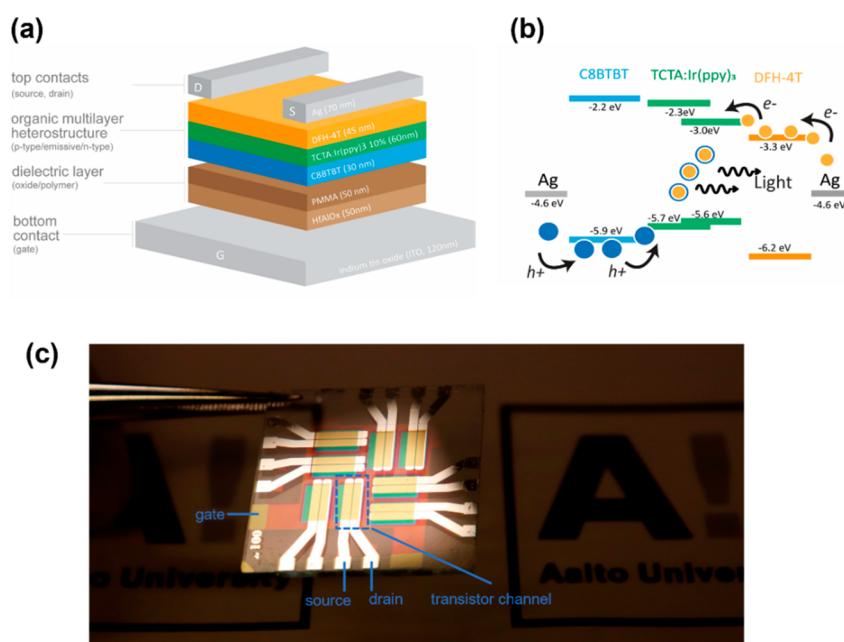


Figure 3. Organic light-emitting transistors (OLETs). (a) Schematics and (b) energy levels of the multilayer structure in our organic light-emitting transistors. (c) Optical image of one of our representative substrates, with electrode and channel labeled accordingly (see the text for details).

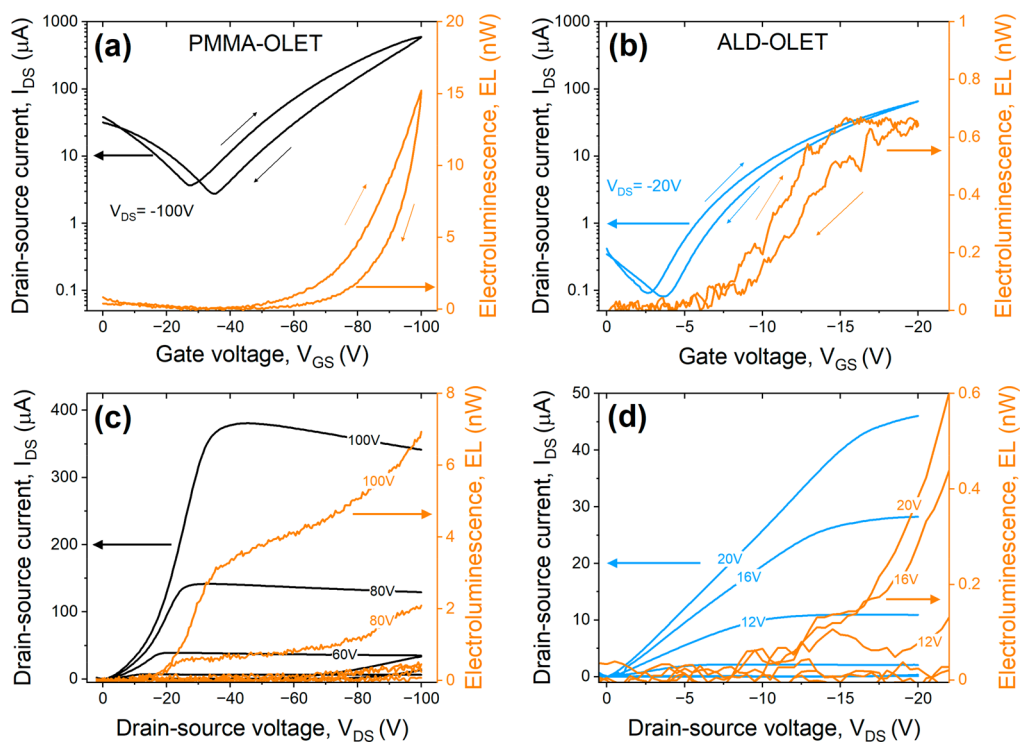


Figure 4. Optoelectronic characterization of OLET with different dielectric layers. (a, b) Saturation transfer curves (I_{DS} vs V_{GS}) for PMMA-OLET ($V_{DS} = -100$ V) and ALD-OLET ($V_{DS} = -20$ V) and (c, d) corresponding multiple output curves. Drain–source and gate voltage values as well as sweep directions are also indicated. Right y-axis shows the electroluminescence measured through the substrate (see the text for details).

OLET, with maximum applied voltages of $|100|$ and $|20|$ V, respectively.

Figures 4a and 4b show the transfer characteristics (p-type) of our organic light-emitting transistors, which presents the typical “V”-shape, suggesting that both devices are operating in an ambipolar regime. We found somehow a balanced device charge transport within the applied bias range, with hole transport being the dominant mechanism and hole currents

approximately one (two) order(s) of magnitude larger than the electron contribution in PMMA(ALD)-OLET. Considering the multilayer structure (see Figure 3a), the operation in our ambipolar devices can be seen as the vertical stack of two organic thin-film transistors, connected in parallel with each carrying one type of charge (holes or electrons) toward the intermediate layer for recombination and emission. As V_{GS} is increased (at a constant source–drain bias), light generation

can occur when (only) holes are injected and transported in the device (i.e., right side of I_{DS} curve) or when both single charge transistors are operating (ON-state, around the I_{DS} apex). In the case of relatively balanced charge distributions, when minority charges (n-type semiconductor) are injected toward the recombination area, the drain–source current (in saturation) can be then written as

$$I_{DS,sat} = \frac{W}{2L} [\mu_{e,sat} C_i (V_{GS} - V_{th,e})^2 + \mu_{h,sat} C_i (V_{DS} - (V_{GS} - V_{th,h}))^2] \quad (2)$$

where W (5 mm) and L (100 μm) are the transistor channel width and length, C_i is the capacitance per unit area of the gate dielectric ($C_{i,HfAlO_x/PMMA} = 63 \text{ nF/cm}^2$, $C_{i,PMMA} = 6.6 \text{ nF/cm}^2$), and V_{th} and μ_{sat} are the threshold bias and mobility for holes (h) and electrons (e), respectively.

Before discussing in more details our results, we here note the following: (i) we observed no evident difference in morphology or structure of the active region depending on underlying dielectric surface (see Figure S4); (ii) transistors fabricated on HfAlO_x film-only or bilayer dielectric stack with HfAlO_x thicknesses $<50 \text{ nm}$ show a high level of leakage current; and (iii) vertical fields (at the organic interface) in PMMA- and ALD-OLET are very similar ($E_{GS,PMMA} = V_{GS,PMMA}/t_{PMMA} = 2.2 \text{ MV/cm} \sim E_{GS,ALD} = V_{GS,ALD}/t_{ALD} = 2 \text{ MV/cm}$), while the horizontal field in PMMA-OLET is 5 times larger than ALD-OLET ($E_{PMMA}/E_{ALD} = V_{DS,PMMA}/V_{DS,ALD} = 5$, in the limit of the same channel length).

As expected, using a higher capacitance gate dielectric ($\text{HfAlO}_x/\text{PMMA}$) enables lower driving conditions (1100 \rightarrow 201 V), along with a reduction in threshold voltage (136 \rightarrow 61 V), with corresponding light emission within similar range. These values are consistent with available literature for transistors using PMMA and high- k materials (oxides).⁵⁸ Our devices present negligible values of gate leakage currents (\sim few nA) within their bias range of operation (at least 3 orders of magnitude smaller than the largest drain–source current). This is a key advantage for applications where reduced power consumption and compatibility with commercial IC unit are required.

Table 1 summarizes the figures of merit of our organic light-emitting transistors. The field-effect mobility and threshold voltage are calculated from the linear fit of $\sqrt{\frac{2L}{WC_i} I_{DS,sat}}$ sweep of the locus curves (I_{DS} vs $V_{GS} = V_{DS}$) for both holes and electrons (see Figure S5). We found average values for hole and electron mobilities of ~ 0.2 and $\sim 0.003 \text{ cm}^2/(\text{V s})$ for the ALD-based OLET and ~ 1 and $\sim 0.1 \text{ cm}^2/(\text{V s})$ for the PMMA, respectively. These are smaller (~ 1 order of magnitude) than values found in single-layer organic field-effect transistor (based on PMMA dielectric); for more details, we refer the reader to ref 25. This difference reflects the difference in the capacitance value and bias conditions, where

$$\frac{\mu_{sat,PMMA}}{\mu_{sat,ALD}} = \frac{\sqrt{\frac{2L}{WC_{i,PMMA}} I_{DS,sat,PMMA}}}{\sqrt{\frac{2L}{WC_{i,ALD}} I_{DS,sat,ALD}}} = \sqrt{\frac{C_{i,ALD} V_{DS,PMMA}}{C_{i,PMMA} V_{DS,ALD}}} \sim 6.9$$

It has been previously reported that when comparing carrier mobilities from different dielectric materials, lower values were obtained with high- k oxides. This is mainly attributed to polar modes affecting scattering and thus mobility at lower and

Table 1. Optoelectronic Properties of Organic Light-Emitting Transistors with Different Dielectrics^a

		PMMA-OLET	ALD-OLET
gate dielectric (material)	–	PMMA	$\text{HfAlO}_x/\text{PMMA}$
dielectric thickness	nm	440	50/50
capacitance/unit area, C_i	nF/cm ²	6.6	63
dielectric permittivity, k	–	3.3	7.1
max driving bias, V_{max}	V	100	20
max drain-source current, $I_{DS,max}$	μA	600	66
max electroluminescence, EL_{max}	nW	15.2	0.65
hole mobility, $\mu_{h,sat}$	cm ² /(V s)	1.09	0.19
hole threshold, $V_{h,th}$	V	–35.7	–6.2
electron mobility, $\mu_{e,sat}$	cm ² /(V s)	0.08	0.003
electron threshold, $V_{e,th}$	V	43.8	12.9
ON/OFF ratio	–	1.4×10^5	1.5×10^4
subthreshold slope, SS	V/dec	22.1	2.6
max external quantum efficiency (at $V_{DS,max}$), EQE_{max}	$\times 10^{-3}\%$	1.1	0.45

^aSummary of the figures of merit of the organic light-emitting transistors using as dielectrics bilayer stack (ALD-OLET) and PMMA (PMMA-OLET), the latter considered as reference. Mobility and threshold values are extracted from locus curve (I_{DS} vs $V_{GS} = V_{DS}$) while maximum current, ON/OFF ratio, light output (EL), and EQE are extracted from the transfer curves in Figures 4a and 4b and corresponding to $V_{DS} = |V_{DS,max}| = 20$ (100) V for ALD- (PMMA-) organic light-emitting transistors.

moderate gate fields.^{59,33} Such mobility variation can partially arise from the larger ionic polarization nature of high- k materials (related to metal–oxygen bonds which are associated with energy lattice oscillations), resulting in a larger scattering strength.^{60,61} In our case, combining a high- k dielectric with a low- k insulator might also reduce energetic disorder (in high- k materials random dipoles affect the energy of localized states leading to higher energetic disorder and thus to a variation in mobility).⁶²

Figures 4c and 4d show the multiple output curves for our devices, both characterized by an initial linear current increase ($|V_{GS}|$ as labeled in the panels), followed by saturation, beyond the channel pinch-off point. The measured emitted light corresponding to these curves suggests a limited contribution coming from the electron transport, with the device operating in unipolar regime for $|V_{DS}| < |V_{GS}|$ and more ambipolar for $|V_{DS}| > |V_{GS}|$ (see Figure S5 for unipolar behavior and Figure S7 for light emission in our devices).

We here note that devices on the same substrate show a variation of hole and electron currents in the range of 10–15%, closely reflected onto an estimate of figure of merits, such as threshold and mobilities (Figure S6). Table 1 also includes the values for the external quantum efficiency for which we observed a difference between ALD- and PMMA-OLET devices, arising from the different bias conditions (horizontal field mainly) and the different degrees of ambipolarity (Figures 4a and 4b) in the two devices. In particular, the lower value for the ALD-OLET might result from limited electron current as well as light generated close to the drain electrode. This might lead to increased charge-exciton quenching, hindering an efficient light extraction process. Also, phenomena such as enhanced charge injection, improved interfaces, and energy and charge transfer in the emissive layer might play a significant role.⁶³ Additionally, the EQE values are expectedly

underestimated, given that the measured light (bottom emission) is only a part of the total light generated in the device. For a more detailed analysis of these emissive blends in terms of optical and optoelectronic properties in field-effect light-emitting transistors, we refer to one of our recent works.⁵⁷

Further, we also observed non-negligible hysteresis in our devices. Figure S8 summarizes the difference in drain–source current measured at fixed current between the forward and reverse sweeps for both PMMA- and ALD-OLET. We found a shift (toward higher bias) of approximately 10 V in PMMA-OLET and about 1 V in ALD-OLET, when V_{DS} (or V_{GS}) is smaller than the maximum applied bias V_{max} . While a detailed investigation is currently in progress and beyond the scope of the present article, we expect charge trapping localized at the dielectric interface and the different charge transport and injection regimes to be relevant phenomena.⁵⁴ Generally, in devices with metal oxide and hybrid dielectric, field-effect transistors behavior might be affected by (a) charges injected from the gate into the dielectric, and consequently trapped inside the dielectric,⁶⁴ (b) residual dipoles in the bulk of the dielectric, which can possibly be reoriented by an external field,⁶⁵ and (c) trapped carriers in the channel–dielectric interface often related to electrons trapped to hydroxyl groups (OH) at such an interface.⁶⁶ While all three mechanisms can potentially contribute, the most dominant mechanism will determine the magnitude of hysteresis in the transistor with a certain bilayer dielectric. Based on the negligible leakage current in our experimental findings, we can neglect contribution coming from (a); thus, we anticipate that (b) and (c) can contribute in a similar way, with (b) likely plausible in the case of PMMA dielectric fabrication process (i.e., given the larger thickness of PMMA). Further, trapped charges can also affect indirectly the contact properties while limiting the injection by building up a space charge region adjacent to the contacts.⁶⁷ This can limit the number of available mobile charges, and thus the mobility,⁶⁸ with the latter one relevant for coplanar device configuration and for multilayer active region with the charge injection occurring at the contact edge (\sim tens of nanometers).⁶⁹ In our multilayer architecture, charge injection occurs at the contact area with the gate (\sim tens of micrometers), with the transport through the semiconductor layer can contribute to the contact resistance⁷⁰ and partial screening of the gate field. Moreover, the dielectric/OSC interface (PMMA/C8BTBT) is similar in both of our devices (minor differences cannot be excluded because PMMA solutions are different and thus might lead to local fields/dipole variation at the interface). Charges move along the semiconductor/insulator interface (thin accumulation layer)² and the gate dielectric can affect the transport within the channel by modifying the overall morphology of semiconductor layer, trap densities at the interface, or the energetic disorder induced by the dielectric internal dipole in the semiconductor.⁶⁰

Further, we cannot *a priori* exclude that the hysteresis and its amplitude depend on measurement parameters (i.e., sweeping rate, applied gate bias range), as is well-known in transistor technology. Further, the Al_2O_3 film grown by ALD exhibits reduced hysteresis from decrease trapped charge.³⁹ We also calculated the interface trap density as follows:

$$D_{it} = \frac{C_i}{q} \left(\frac{qSS \log e}{kT} - 1 \right) \quad (3)$$

where SS is the subthreshold slope (defined as the bias needed to vary the drain–source current by one decade), q is the electron charge, k is Boltzmann's constant, and T is the temperature ($kT \sim 26$ meV at room temperature). The subthreshold slope is obtained by taking the linear fit of the steepest part of the subthreshold region of the plot $\log I_{DS}$ vs V_{GS} ($SS = \frac{dV_{GS}}{d \log I_{DS}}$), with a lower value for SS for a given change in voltage implying a faster increase in current. With values of 22.06 V/decade for PMMA-OLET and 2.63 V/decade for the ALD-OLET, we estimated the density of interface traps to be $1.5 \times 10^{13}/\text{eV cm}^2$ and $1.7 \times 10^{13}/\text{eV cm}^2$, respectively.

These traps will capture charges, preventing them from participating in both the conduction and exciton formation process; these charges can then detrapp when subjected to an external electric field. While the dynamics of trapping/detrapping of charges is currently under investigation and beyond the scope of this work, we believe there is a close link between mobility and interface traps in high- k materials. In fact, higher interface trap density shows lower values of mobility, indicating that Coulomb scattering is also a mechanism taking place in mobility degradation.⁶¹

CONCLUSION

In this work, we have studied and characterized the dielectric properties of a bilayer stack composed of an ALD-based oxide (HfAlO_x, mixture of alumina and hafnia) and a polymeric dielectric (PMMA). In addition, we have implemented this bilayer stack as a gate dielectric for the fabrication of organic light-emitting transistors. We demonstrate that such a dielectric can enable device operation in the voltage range below 20 V, a critical characteristic for the development of low-power consumption devices. When compared to the reference device that uses a single-layer polymeric dielectric, this voltage is 6 times smaller. Our work demonstrated that high- k oxides grown by ALD in combination with polymer dielectrics offer a good compromise between high capacitance density and enhanced interfacial compatibility.

ASSOCIATED CONTENT

Supporting Information

The Supporting Information is available free of charge at <https://pubs.acs.org/doi/10.1021/acsaelm.3c01813>.

Optical properties of HfAlO_x layers with different thickness (Figure S1); surface morphology of bilayer dielectric films (HfAlO_x 50 nm/PMMA 50 nm) (Figure S2); estimate of the dielectric permittivity of HfAlO_x layer; contact angle measurement of PMMA dielectric (Figure S3); surface morphology of organic multilayer heterostructure (on different dielectrics) (Figure S4); electronic characterization of OLET with different dielectric films (Figure S5); variability of figures of merit for organic light-emitting transistors (Figure S6); light emission in organic light-emitting transistor (Figure S7); hysteresis in organic light-emitting transistors (Figure S8) (PDF)

AUTHOR INFORMATION

Corresponding Authors

Katherine Gallegos-Rosas – Department of Electronics and Nanoengineering, School of Electrical Engineering, Aalto

University, 02150 Espoo, Finland; orcid.org/0000-0001-8561-5722; Email: katherine.gallegosrosas@aalto.fi

Caterina Soldano – Department of Electronics and Nanoengineering, School of Electrical Engineering, Aalto University, 02150 Espoo, Finland; orcid.org/0000-0001-6345-290X; Email: caterina.soldano@aalto.fi

Authors

Pia Myllymäki – Beneq Oy, 02200 Espoo, Finland

Mikael Saarniheimo – Beneq Oy, 02200 Espoo, Finland

Sami Sneek – Beneq Oy, 02200 Espoo, Finland

Ramesh Raju – Department of Electronics and Nanoengineering, School of Electrical Engineering, Aalto University, 02150 Espoo, Finland; orcid.org/0000-0002-1802-9077

Complete contact information is available at:
<https://pubs.acs.org/10.1021/acsaelm.3c01813>

Author Contributions

C.S. and K.G.-R. contributed equally to this work. The manuscript was written through the contribution of all authors. All authors have given approval to the final version of the manuscript.

Notes

The authors declare no competing financial interest.

ACKNOWLEDGMENTS

The authors acknowledge the support from the Research Council of Finland Flagship Program PREIN (Grant No. 320167) and Micronova Nanofabrication Centre, Espoo, Finland, within the OtaNano research infrastructure at Aalto University. C.S. and K.G.-R. acknowledge financial support from the Research Council of Finland (WALLPAPER: Grant No. 352914 and EHIR: Grant No. 334487) and from Foundation for Aalto University Science and Technology (Aalto-yliopiston tekniikan tukisäätiö sr). R.R. acknowledges the financial support from the Research Council of Finland (CarbonSurf: Grant No. 329406).

REFERENCES

- (1) Horowitz, G. Organic field-effect transistors. *Adv. Mater.* **1998**, *10*, 365–377.
- (2) Muccini, M.; Koopman, W.; Toffanin, S. The photonic perspective of organic light-emitting transistors. *Laser and Photonics Rev.* **2012**, *6*, 258–275.
- (3) Muccini, M.; Toffanin, S. *Organic Light-Emitting Transistors: Towards the Next Generation Display Technology*; John Wiley & Sons: Hoboken, NJ, 2016.
- (4) Pan, Z.; Liu, K.; Miao, Z.; Guo, A.; Wen, W.; Liu, G.; Liu, Y.; Shi, W.; Kuang, J.; Bian, Y.; Qin, M.; et al. Van der Waals Multilayer Heterojunction for Low-Voltage Organic RGB Area-Emitting Transistor Array. *Adv. Mater.* **2023**, *35* (8), 2209097.
- (5) Capelli, R.; Toffanin, S.; Generali, G.; Usta, H.; Facchetti, A.; Muccini, M. Organic light-emitting transistors with an efficiency that outperforms the equivalent light-emitting diodes. *Nat. Mater.* **2010**, *9*, 496–503.
- (6) Bachelet, A.; Chabot, M.; Ablat, A.; Takimiya, K.; Hirsch, L.; Abbas, M. Low voltage operating organic light emitting transistors with efficient charge blocking layer. *Org. Electron.* **2021**, *88*, 106024.
- (7) McCarthy, M. A.; Liu, B.; Donoghue, E. P.; Kravchenko, I.; Kim, D. Y.; So, F.; Rinzler, A. G. Low-voltage, low-power, organic light-emitting transistors for active matrix displays. *Science*. **2011**, *332* (6029), 570–573.
- (8) Gwinner, M. C.; Kabra, D.; Roberts, M.; Brenner, T. J.; Wallikewitz, B. H.; McNeill, C. R.; Friend, R. H.; Sirringhaus, H.

Highly efficient single-layer polymer ambipolar light-emitting field-effect transistors. *Adv. Mater.* **2012**, *24* (20), 2728–2734.

(9) Lee, J. H.; Ke, T. H.; Genoe, J.; Heremans, P.; Rolin, C. Overlapping-Gate Organic Light-Emitting Transistors. *Adv. Electron. Mater.* **2019**, *5* (1), 1800437.

(10) Ullah, M.; Tandy, K.; Yambem, S. D.; Aljada, M.; Burn, P. L.; Meredith, P.; Namdas, E. B. Simultaneous enhancement of brightness, efficiency, and switching in RGB organic light emitting transistors. *Adv. Mater.* **2013**, *25* (43), 6213–6218.

(11) Muhieddine, K.; Ullah, M.; Pal, B. N.; Burn, P.; Namdas, E. B. All Solution-Processed, Hybrid Light Emitting Field-Effect Transistors. *Adv. Mater.* **2014**, *26* (37), 6410–6415.

(12) Bronstein, H.; Nielsen, C. B.; Schroeder, B. C.; McCulloch, I. The role of chemical design in the performance of organic semiconductors. *Nat. Rev. Chem.* **2020**, *4*, 66–77.

(13) Liu, Y.; Li, C.; Ren, Z.; Yan, S.; Bryce, M. R. All-organic thermally activated delayed fluorescence materials for organic light-emitting diodes. *Nat. Rev. Mater.* **2018**, *3*, 18020.

(14) Soldano, C. Engineering dielectric materials for high-performance organic light-emitting transistors (OLETs). *Materials*. **2021**, *14*, 3756.

(15) Wilk, G. D.; Wallace, R. M.; Anthony, J. M. High-k gate dielectrics: current status and materials properties considerations. *J. Appl. Phys.* **2001**, *89*, S243–S275.

(16) Huang, T. S.; Su, Y. K.; Wang, P. C. Poly (methyl methacrylate) dielectric material applied in organic thin film transistors. *Jpn. J. Appl. Phys.* **2008**, *47* (4S), 3185.

(17) Park, H.; Yoo, S.; Ahn, H.; Bang, J.; Jeong, Y.; Yi, M.; Won, J. C.; Jung, S.; Kim, Y. H. Low-temperature solution-processed soluble polyimide gate dielectrics: from molecular-level design to electrically stable and flexible organic transistors. *ACS Appl. Mater. Interfaces*. **2019**, *11* (49), 45949–45958.

(18) Tetzner, K.; Bose, I. R.; Bock, K. Organic field-effect transistors based on a liquid-crystalline polymeric semiconductor using SU-8 gate dielectrics on flexible substrates. *Materials*. **2014**, *7* (11), 7226–7242.

(19) Raghuvanshi, V.; Bharti, D.; Mahato, A. K.; Varun, I.; Tiwari, S. P.; UV cured PVP gate dielectric for Flexible Organic Field Effect Transistors. *IEEE International Conference on Flexible and Printable Sensors and Systems (FLEPS)*, 2019; pp 1–3.

(20) Campbell, S. A.; Gilmer, D. C.; Wang, X. C.; Hsieh, M. T.; Kim, H. S.; Gladfelter, W. L.; Yan, J. MOSFET transistors fabricated with high permittivity TiO₂ dielectrics. *IEEE Trans. Electron Devices* **1997**, *44* (1), 104–109.

(21) Ortiz, R. P.; Facchetti, A.; Marks, T. J. High-k organic, inorganic, and hybrid dielectrics for low-voltage organic field-effect transistors. *Chem. Rev.* **2010**, *110* (1), 205–239.

(22) Fumagalli, L.; Natali, D.; Sampietro, M.; Peron, E.; Perissinotti, F.; Tallarida, G.; Ferrari, S. Al₂O₃ as gate dielectric for organic transistors: Charge transport phenomena in poly-(3-hexylthiophene) based devices. *Org. Electron.* **2008**, *9* (2), 198–208.

(23) Soldano, C.; Generali, G.; Cianci, E.; Tallarida, G.; Fanciulli, M.; Muccini, M. Organic Light Emitting Transistors (OLETs) using ALD-grown Al₂O₃ dielectric. *SID Symposium Digest of Technical Papers*. **2016**, *47* (1), 1737–1739.

(24) Soldano, C.; D'Alpaos, R.; Generali, G. Highly efficient red organic light-emitting transistors (OLETs) on high-k dielectric. *ACS Photonics*. **2017**, *4* (4), 800–805.

(25) Albeltagi, A.; Gallegos-Rosas, K.; Soldano, C. High-k fluoropolymers dielectrics for low-bias ambipolar organic light-emitting transistors (OLETs). *Materials*. **2021**, *14* (24), 7635.

(26) Gieraltowska, S.; Wachnicki, L.; Witkowski, B. S.; Godlewski, M.; Guzewicz, E. Properties of thin films of high-k oxides grown by atomic layer deposition at low temperature for electronic applications. *Opt. Appl.* **2013**, *43* (1), 17–25.

(27) Wang, B.; Huang, W.; Chi, L.; Al-Hashimi, M.; Marks, T. J.; Facchetti, A. High-k gate dielectrics for emerging flexible and stretchable electronics. *Chem. Rev.* **2018**, *118* (11), 5690–5754.

(28) Groner, M. D.; Elam, J. W.; Fabreguette, F. H.; George, S. M. Electrical characterization of thin Al₂O₃ films grown by atomic layer

- deposition on silicon and various metal substrates. *Thin Solid Films*. **2002**, *413* (1–2), 186–197.
- (29) Gaskins, J. T.; Hopkins, P. E.; Merrill, D. R.; Bauers, S. R.; Hadland, E.; Johnson, D. C.; Koh, D.; Yum, J. H.; Banerjee, S.; Nordell, B. J.; Paquette, M. M.; Caruso, A. N.; Lanford, W. A.; Henry, P.; Ross, L.; Li, H.; Li, L.; French, M.; Rudolph, A. M.; King, S. W. Investigation and review of the thermal, mechanical, electrical, optical, and structural properties of atomic layer deposited high-k dielectrics: Beryllium oxide, aluminum oxide, hafnium oxide, and aluminum nitride. *ECS J. Solid State Sci. and Technol.* **2017**, *6* (10), 189–208.
- (30) Yue, Y.; Hao, Y.; Zhang, J.; Ni, J.; Mao, W.; Feng, Q.; Liu, L. AlGaIn/GaN MOS-HEMT With HfO₂ Dielectric and Al₂O₃ Interfacial Passivation Layer Grown by Atomic Layer Deposition. *IEEE Electron Device Lett.* **2008**, *29* (8), 838–840.
- (31) Park, K. Y.; Cho, H. I.; Choi, H. C.; Bae, Y. H.; Lee, C. S.; Lee, J. L.; Lee, J. H. Device characteristics of AlGaIn/GaN MIS-HFET using Al₂O₃–HfO₂ laminated high-k dielectric. *Jpn. J. Appl. Phys.* **2004**, *43* (11A), 1433–1435.
- (32) Fohlerova, Z.; Mozalev, A. Anodic formation and biomedical properties of hafnium-oxide nanofilms. *J. Mater. Chem. B* **2019**, *7* (14), 2300–2310.
- (33) Robertson, J. Interfaces and defects of high-k oxides on silicon. *Solid-State Electron.* **2005**, *49* (3), 283–293.
- (34) Park, P. K.; Kang, S. W. Enhancement of dielectric constant in HfO₂ thin films by the addition of Al₂O₃. *Appl. Phys. Lett.* **2006**, *89* (19), 192905.
- (35) Auciello, O.; Fan, W.; Kabius, B.; Saha, S.; Carlisle, J. A.; Chang, R. P. H.; Lopez, C.; Irene, E. A.; Baragiola, R. A. Hybrid titanium–aluminum oxide layer as alternative high-k gate dielectric for the next generation of complementary metal–oxide–semiconductor devices. *Appl. Phys. Lett.* **2005**, *86* (4), 042904.
- (36) Groner, M. D.; Fabreguette, F. H.; Elam, J. W.; George, S. M. Low-temperature Al₂O₃ atomic layer deposition. *Chem. Mater.* **2004**, *16* (4), 639–645.
- (37) Hirvikorpi, T.; Laine, R.; Vaha-Nissi, M.; Kilpi, V.; Salo, E.; Li, W.-M.; Lindfors, S.; Vartiainen, J.; Kentta, E.; Nikkola, J.; Harlin, A.; Kostamo, J. Barrier properties of plastic films coated with an Al₂O₃ layer by roll-to-roll atomic layer deposition. *Thin Solid Films*. **2014**, *550*, 164–169.
- (38) Kim, H.; Lee, H.-B.-R.; Maeng, W.-J. Applications of atomic layer deposition to nanofabrication and emerging nanodevices. *Thin Solid Films*. **2009**, *517* (8), 2563–2580.
- (39) Zhang, X. H.; Domercq, B.; Wang, X.; Yoo, S.; Kondo, T.; Wang, Z. L.; Kippelen, B. High-performance pentacene field-effect transistors using Al₂O₃ gate dielectrics prepared by atomic layer deposition (ALD). *Org. Electron.* **2007**, *8* (6), 718–726.
- (40) Wang, C. Y.; Fuentes-Hernandez, C.; Yun, M.; Singh, A.; Dindar, A.; Choi, S.; Graham, S.; Kippelen, B. Organic field-effect transistors with a bilayer gate dielectric comprising an oxide nanolaminate grown by atomic layer deposition. *ACS Appl. Mater. Interfaces.* **2016**, *8* (44), 29872–29876.
- (41) Kim, G.; Fuentes-Hernandez, C.; Jia, X.; Kippelen, B. Organic thin-film transistors with a bottom bilayer gate dielectric having a low operating voltage and high operational stability. *ACS Appl. Electron. Mater.* **2020**, *2* (9), 2813–2818.
- (42) Tian, F.; Chor, E. F. Improved electrical performance and thermal stability of HfO₂/Al₂O₃ bilayer over HfO₂ gate dielectric AlGaIn/GaN MIS–HFETs. *J. Electrochem. Soc.* **2010**, *157* (5), 557–561.
- (43) Cho, M. H.; Choi, C. H.; Seul, H. J.; Cho, H. C.; Jeong, J. K. Achieving a low-voltage, high-mobility IGZO transistor through an ALD-derived bilayer channel and a hafnia-based gate dielectric stack. *ACS Appl. Mater. Interfaces.* **2021**, *13* (14), 16628–16640.
- (44) Zhao, X.; Vanderbilt, D. Phonons and lattice dielectric properties of zirconia. *Phys. Rev. B* **2002**, *65* (7), 075105.
- (45) Lee, P. F.; Dai, J. Y.; Wong, K. H.; Chan, H. L. W.; Choy, C. L. Growth and characterization of Hf–aluminate high-k gate dielectric ultrathin films with equivalent oxide thickness less than 10 Å. *J. Appl. Phys.* **2003**, *93* (6), 3665–3667.
- (46) Katamreddy, R.; Inman, R.; Jursich, G.; Soulet, A.; Takoudis, C. Effect of film composition and structure on the crystallization point of atomic layer deposited HfAlOx using metal (diethylamino) precursors and ozone. *Acta Mater.* **2008**, *56* (4), 710–718.
- (47) Kull, M.; Piirsoo, H. M.; Tarre, A.; Mändar, H.; Tamm, A.; Jõgiaas, T. Hardness, Modulus, and Refractive Index of Plasma-Assisted Atomic-Layer-Deposited Hafnium Oxide Thin Films Doped with Aluminum Oxide. *Nanomaterials.* **2023**, *13* (10), 1607.
- (48) Liu, C.; Xu, Y.; Li, Y.; Scheideler, W.; Minari, T. Critical impact of gate dielectric interfaces on the contact resistance of high-performance organic field-effect transistors. *J. Phys. Chem. C* **2013**, *117* (23), 12337–12345.
- (49) Deman, A. L.; Tardy, J. J. PMMA–Ta₂O₅ bilayer gate dielectric for low operating voltage organic FETs. *Org. Electron.* **2005**, *6* (2), 78–84.
- (50) Jang, J.; Nam, S.; Yun, W. M.; Yang, C.; Hwang, J.; An, T. K.; Chung, D. S.; Park, C. E. High Tg cyclic olefin copolymer/Al₂O₃ bilayer gate dielectrics for flexible organic complementary circuits with low-voltage and air-stable operation. *J. Mater. Chem. A* **2011**, *21* (33), 12542–12546.
- (51) Alshammari, F. H.; Nayak, P. K.; Wang, Z.; Alshareef, H. N. Enhanced ZnO thin-film transistor performance using bilayer gate dielectrics. *ACS Appl. Mater. Interfaces.* **2016**, *8* (35), 22751–22755.
- (52) Hung, L. S.; Chen, C. H. Recent progress of molecular organic electroluminescent materials and devices. *Mater. Sci. Eng. R Rep.* **2002**, *39* (5–6), 143–222.
- (53) Zhang, X. H.; Tiwari, S. P.; Kippelen, B. Pentacene organic field-effect transistors with polymeric dielectric interfaces: Performance and stability. *Org. Electron.* **2009**, *10* (6), 1133–1140.
- (54) Liu, C.; Xu, Y.; Li, Y.; Scheideler, W.; Minari, T. Critical impact of gate dielectric interfaces on the contact resistance of high-performance organic field-effect transistors. *J. Phys. Chem. C* **2013**, *117* (23), 12337–12345.
- (55) Choi, H. H.; Lee, W. H.; Cho, K. Bias-stress-induced charge trapping at polymer chain ends of polymer gate-dielectrics in organic transistors. *Adv. Funct. Mater.* **2012**, *22* (22), 4833–4839.
- (56) Kukli, K.; Kemell, M.; Castan, H.; Duenas, S.; Seemen, H.; Rähn, M.; Link, J.; Stern, R.; Ritala, M.; Leskelä, M. Atomic layer deposition and properties of HfO₂–Al₂O₃ nanolaminates. *ECS J. Solid State Sci. and Technol.* **2018**, *7* (9), 501–508.
- (57) Soldano, C.; Laouadi, O.; Gallegos-Rosas, K. TCTA: Ir(ppy)₃ Green Emissive Blends in Organic Light-Emitting Transistors (OLETs). *ACS Omega.* **2022**, *7* (48), 43719–43728.
- (58) Soldano, C.; Generali, G.; Cianci, E.; Tallarida, G.; Fanciulli, M.; Muccini, M. Engineering organic/inorganic alumina-based films as dielectrics for red organic light-emitting transistors. *Thin Solid Films.* **2016**, *616*, 408–414.
- (59) Virkar, A. A.; Mannsfeld, S.; Bao, Z.; Stingelin, N. Organic semiconductor growth and morphology considerations for organic thin-film transistors. *Adv. Mater.* **2010**, *22* (34), 3857–3875.
- (60) Fischetti, M.; Neumayer, D.; Cartier, E. Effective electron mobility in Si inversion layers in MOS systems with a high-k insulator: The role of remote phonon scattering. *J. Appl. Phys.* **2001**, *90* (9), 4587.
- (61) Zhu, W.; Han, J. P.; Ma, T. P. Mobility measurement and degradation mechanisms of MOSFETs made with ultrathin high-k dielectrics. *IEEE Trans. Electron Devices* **2004**, *51* (1), 98–105.
- (62) Veres, J.; Ogier, S. D.; Leeming, S. W.; Cupertino, D. C.; Mohialdin Khaffaf, S. Low-k insulators as the choice of dielectrics in organic field-effect transistors. *Adv. Funct. Mater.* **2003**, *13* (3), 199–204.
- (63) Kong, L.; Wu, J.; Li, Y.; Cao, F.; Wang, F.; Wu, Q.; Shen, P.; Zhang, C.; Luo, Y.; Wang, L.; Turyanska, L.; Ding, X.; Zhang, J.; Zhao, Y.; Yang, X. Light-emitting field-effect transistors with EQE over 20% enabled by a dielectric-quantum dots-dielectric sandwich structure. *Sci. Bull.* **2022**, *67* (5), 529–536.
- (64) Hwang, D. K.; Lee, K.; Kim, J. H.; Im, S.; Park, J. H.; Kim, E. Comparative studies on the stability of polymer versus SiO₂ gate

dielectrics for pentacene thin-film transistors. *Appl. Phys. Lett.* **2006**, *89* (9), 093507.

(65) Klauk, H., Ed.; *Organic Electronics II: More Materials and Applications*; John Wiley & Sons: 2012; pp 197–225.

(66) Hwang, D. K.; Oh, M. S.; Hwang, J. M.; Kim, J. H.; Im, S. Hysteresis mechanisms of pentacene thin-film transistors with polymer/oxide bilayer gate dielectrics. *Appl. Phys. Lett.* **2008**, *92* (1), 013304.

(67) Natali, D.; Caironi, M. Charge Injection in Solution-Processed Organic Field-Effect Transistors: Physics, Models and Characterization Methods. *Adv. Mater.* **2012**, *24* (11), 1357–1387.

(68) Horowitz, G.; Hajlaoui, M. E.; Hajlaoui, R. Temperature and gate voltage dependence of hole mobility in polycrystalline oligothiophene thin film transistors. *J. Appl. Phys.* **2000**, *87* (9), 4456–4463.

(69) Hallam, T.; Duffy, C. M.; Minakata, T.; Ando, M.; Sirringhaus, H. A scanning Kelvin probe study of charge trapping in zone-cast pentacene thin film transistors. *Nanotechnology*. **2009**, *20* (2), 025203.

(70) Richards, T. J.; Sirringhaus, H. Analysis of the contact resistance in staggered, top-gate organic field-effect transistors. *J. Appl. Phys.* **2007**, *102* (9), 094510.